

*Regular article*

# Effective modeling of intrinsic and environmental effects on the structure and electron paramagnetic resonance parameters of nitroxides by an integrated quantum mechanical/molecular mechanics/polarizable continuum model approach

R. Improta<sup>1</sup>, A. di Matteo<sup>2</sup>, V. Barone<sup>1</sup>

<sup>1</sup>Dipartimento di Chimica, Università Federico II, Via Mezzocannone 4, 80134 Naples, Italy

<sup>2</sup>Dipartimento di Chimica Fisica, Università di Padova, Via Loredan 2 Padua, Italy

Received: 17 September 1999 / Accepted: 3 February 2000 / Published online: 29 June 2000

© Springer-Verlag 2000

**Abstract.** Experimental and density functional theory geometries have been used to extend the AMBER force field to nitroxides. An optimum set of transferable atomic charges for the calculation of electrostatic interactions both in vacuo and in aqueous solution has been obtained by averaging the charges obtained by a restrained electrostatic potential fitting of representative compounds. Besides reliable structural data, our implementation allows the computation of accurate spectromagnetic properties by single-point B3LYP computations on geometries optimized at the AMBER level. Solvent shifts in aqueous solution can be reproduced quantitatively by a mixed model in which specific solvent effects are described by two water molecules strongly coordinated to the nitroxide oxygen, while bulk effects are described by the polarizable continuum model.

**Key words:** Electron spin resonance – Nitroxides – Quantum mechanical/molecular mechanics methods

## 1 Introduction

Chemical inertness [1] coupled to the strong localization of the unpaired spin in the NO moiety [2] makes nitroxides the class of organic free radicals most widely used as “spin probes” [3] for the study of the structure and the dynamics of microheterogeneous macromolecular systems such as micelles [4], proteins [5] and vesicles [6] by means of electron spin resonance (ESR) spectroscopy. Since the magnitude of the isotropic hyperfine splitting (hfs) of the nitroxide nitrogen ( $A_N$ ) depends remarkably on the polarity of the solvent [7], nitroxides

are indeed ideal “probes” of the micropolarity of the medium in which they are embedded. Furthermore, the line widths of the ESR spectra (and the effective rotational correlation time,  $\tau$ ) are controlled by the rotational and lateral diffusion of the nitroxide and can give valuable information on the viscosity, the degree of order and the temperature of the spin probe environment [8].

Just to mention a few examples, nitroxides have been successfully used to determine the location of organic compounds in micelles [9], to determine the structure and the fluidity of lipid bilayers [10] and to study the interaction between polymers and surfactants [11].

The stability of the nitroxide radicals and their importance as spin probes have given spur to many experimental studies addressed to the assessment of the dependence of  $A_N$  on the geometry of the nitroxide [12] and on the solvent polarity [7]. Notwithstanding this, several questions are still open and deserve a deeper investigation, such as the one raised by an ad hoc quantum mechanical (QM) study. These involve, for instance, the definition of the main factors which determine the magnitude of  $A_N$ , an evaluation of their relative importance and, eventually, a clear-cut separation of intrinsic and environmental contributions. From this point of view, methods rooted in density functional theory (DFT) have already provided trends in very good agreement with the experimental ones [13, 14], if the effect of the solvent is taken into account by the use of the so-called polarizable continuum model (PCM) [15, 16]. However, the chemical stability of the nitroxides and their use as spin probes often require the presence of large substituents on the nitroxide moiety [3], leading to species which, due to their size, can hardly be tackled by sophisticated QM techniques. An effective way out from this problem is provided by the “integrated” use of QM and molecular mechanics (MM) methods. To this end we have recently extended some popular force fields (MM+ and UFF) to nitroxides, obtaining geometrical parameters in good

Correspondence to: R. Improta  
e-mail: robimp@chemna.dichi.unina.it

agreement with experiments and ab initio calculations, both in vacuo and in condensed phases [13]. However, an increase in the number of the experimental and QM reference data for the fitting of the MM parameters is very useful to improve their reliability for several different classes of nitroxides. In particular, we will be concerned with the AMBER force field [17], which is specifically tailored for the study of biological systems and is included in several commercial packages: it is thus a very good candidate for the implementation of effective QM/MM methods and for their use in the study of the interaction of nitroxides with biological macromolecules.

In this article we extend the AMBER force field to nitroxides and report the results of a DFT/MM/PCM study of three representative members of this class, namely pyrrolidine-1-oxyl (hereafter I), pyrroline-1-oxyl (II) and imidazoline-1-oxyl (III) (Fig. 1). In these compounds the NO moiety is part of a five-membered ring, one of the class of nitroxides which has been most used as spin probes [3].

## 2 Computational details

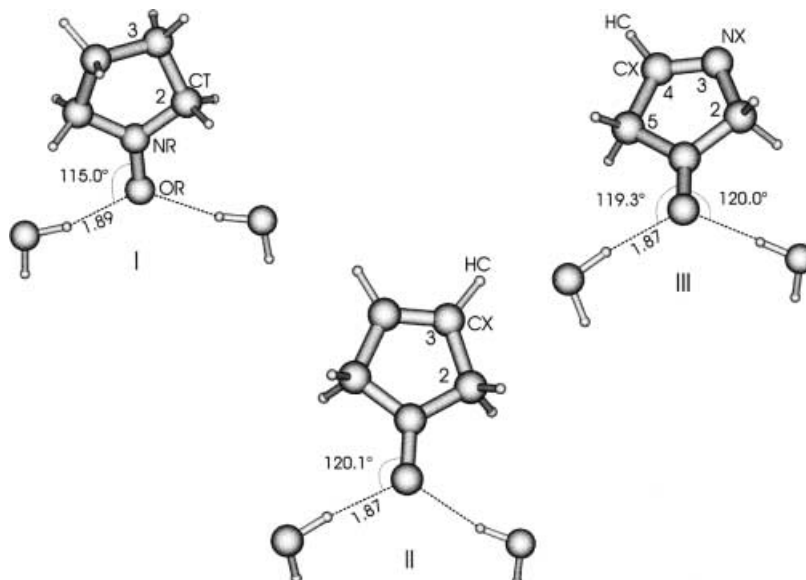
All the QM computations are based on the unrestricted Kohn–Sham (UKS) approach to DFT [18], selecting (on the grounds of previous experience) [19] the B3LYP hybrid functional [20]. The standard 6-31G\* basis set [21] was used for the geometry optimizations, whereas the magnetic properties were computed by the purposely developed EPR-2 basis set [22].

The isotropic hfs of the nitroxide nitrogen is calculated by means of Eq. (1) [23]

$$A_N = \frac{8}{3}\pi g_n g_e \mu_n \mu_e \rho_s(r_N) , \quad (1)$$

where  $\mu_n$  and  $g_n$  are the nuclear magneton and nuclear  $g$  factors, respectively. The term  $g_e$  is the  $g$  value for the electron (in the present work  $g_e = 2.0$ ),  $\mu_e$  is the Bohr magneton and  $\rho_s(r_N)$  is the electronic spin density at the nitrogen nucleus.

**Fig. 1.** Schematic drawing, numbering and types of atoms for the three compounds considered in the present work, together with the water molecules strongly coordinated to the NO group



Solvent effects were evaluated by using the PCM [15, 16], which is based on a self-consistent description of a molecule embedded in a cavity surrounded by an infinite dielectric. The cavity is defined in terms of spheres centered on non-hydrogen atoms with radii optimized following the UATM (United Atom Topological Model) [16], which has been shown to reproduce the experimental solvation free energy of many neutral and charged solutes.

All the QM calculations were performed using the GAUSSIAN98 package [24], whereas the MM computations were performed using the AMBER force field [17], available in the Hyperchem package [25].

## 3 Results and discussion

### 3.1 MM computations

The geometries of the three compounds under study were optimized in vacuo at the B3LYP/6-31G\* level (Tables 1, 2). From the experimental and the QM geometries we then derived the parameters shown in Table 3, using the procedure presented in detail in Ref. [13]. All the parameters not explicitly shown in Table 3 have the values optimized in Ref. [13] for the MM+ and UFF force fields.

The introduction of the new parameters in the AMBER force field yields the geometries reported in Tables 1 and 2.

For I and II all the calculated bond lengths are close to their experimental values and, taking into account that the reference experimental compounds bear bulky substituents, there is good agreement also between the calculated and the experimental bond angles. We did not succeed in finding any experimental geometry of derivatives of III however, all the geometrical parameters determined by MM computations are similar to their B3LYP counterparts.

Since we are primarily interested in the evaluation of the electron spin resonance (ESR) parameters of nitr-

**Table 1.** Geometrical parameters (distances in angstroms and angles in degrees) for pyrrolidine-1-oxyl (I) and pyrroline-1-oxyl (II). Atom numbering is shown in Fig. 2

	I			II		
	Exp <sup>a</sup>	B3LYP	AMBER	Exp <sup>b</sup>	B3LYP	AMBER
N1—O1	1.264	1.272	1.281	1.270	1.272	1.281
N1—C2	1.478	1.471	1.470	1.501	1.471	1.472
C2—C3	1.524	1.534	1.529	1.520	1.504	1.498
C3—C3'	1.531	1.546	1.532	1.315	1.336	1.334
C2—N1—C2'	115.3	113.4	115.2	114.5	112.8	113.1
N1—C2—C3	99.9	103.1	102.2	99.0	101.9	102.1
C2—C3—C3'	105.6	103.8	103.8	113.5	111.7	111.3
C2—C3—C3'—C2'	36.6	36.3	36.3	0.00	0.00	0.00
O1—N1—C2—C2'	180.0	180.0	179.4	180.0	180.0	180.0
O1—N1—C2—C3	-162.7	-168.7	-168.1	180.0	-179.7	179.9

<sup>a</sup> Reference compound: 2,2,5,5-tetramethyl-3-hydroxypyrrolidine-1-oxyl [26]

<sup>b</sup> Reference compound: 2,2,5,5-tetramethyl-3-carboxy-pyrroline-1-oxyl [27]

**Table 2.** Geometrical parameters (distances in angstroms and angles in degrees) for imidazoline-1-oxyl (III). Atom numbering is shown in Fig. 2

	B3LYP	AMBER
N1—O1	1.272	1.281
N1—C2	1.477	1.471
N1—C5	1.466	1.444
C4—C5	1.508	1.494
C4—N3	1.277	1.272
N3—C2	1.452	1.453
C2—N1—C5	109.8	111.3
N1—C5—C4	99.5	99.7
C5—C4—N3	116.2	115.2
C2—N3—C4	108.7	109.4
N3—C2—N1	105.6	104.2
C5—C4—N3—C2	0.03	0.25
O1—N1—C2—C5	166.3	171.7

oxides, it is encouraging that the best agreement between experimental and calculated geometrical parameters occurs for the NO moiety. Particularly, since the value of  $A_N$  depends critically on the competition between a pyramidal ( $sp^3$ -like hybridization) and a planar ( $sp^2$ -like hybridization) geometry around the nitrogen atom [28], it is worth noting that all the calculated out-of-plane angles are very close to their experimental counterparts. This important point was overlooked in recent MM parameterization for nitroxide radicals [29].

### 3.2 Atomic point charges

While the structures of isolated nitroxides are scarcely sensitive to electrostatic interactions, the situation is completely different for intermolecular interactions, either with biological substrates or with the solvent [13]. This requires the derivation of reliable atomic point charges which should be easily transferable between common functional groups in related molecules, should not be too conformationally dependent and, at the same time, should accurately reproduce the electrostatic potential around the molecule.

For these reasons we resorted to the restrained electrostatic potential (RESP) procedure [30]. This model is

**Table 3.** Optimized molecular mechanics (MM) parameters involving NR, OR and LP species (see Fig. 1 for atom types)

Bond stretching		$R_o$ (Å)	$K_r$ (kcal mol <sup>-1</sup> Å <sup>-2</sup> )		
OR	NR	1.2800	337.0000		
CX	CX	1.3370	690.0000		
C	CX	1.3510	690.0000		
CT	CX	1.5000	350.0000		
CT	NX	1.4500	414.0000		
CX	NX	1.2700	414.0000		
Angle bendings		$\theta_0$ (deg)	$K_\theta$ (kcal mol <sup>-1</sup> rad <sup>-2</sup> )		
NX	CT	NR	110.0000	80.0000	
CX	CT	NR	109.4700	80.0000	
H1	CT	NR	105.6000	80.0000	
HC	CT	NR	109.5000	50.0000	
NR	OR	LP	120.0000	600.0000	
LP	OR	LP	120.0000	600.0000	
HC	CX	HC	120.0000	46.0000	
CX	CX	HC	120.0000	50.0000	
CT	CX	HC	120.0000	50.0000	
CT	CX	CX	120.0000	70.0000	
CT	CX	NX	125.0000	70.0000	
HC	CX	NX	120.0000	50.0000	
CX	NX	CT	118.0000	70.0000	
Improper torsion		$\phi_0$ (deg)	$K_\phi$ (kcal mol <sup>-1</sup> )		
—	—	NR	OR	180.0000	10.5000
—	—	OR	LP	180.0000	90.5000
Regular torsion		$\tau_0$ (deg)	$V_3/2$ (kcal mol <sup>-1</sup> rad <sup>-2</sup> )		
H1	CT	CT	NR	0.0000	0.3333
CT	NR	OY	LP	180.0000	0.3000
CX	CT	NR	OR	0.0000	0.3333
NX	CT	NR	OR	0.0000	0.3333
H1	CT	NR	OR	0.0000	0.6000
CX	CT	NR	OR	0.0000	0.3333
H1	CT	NR	OR	0.0000	0.6000
—	CX	CX	—	180.0000	10.0000
—	CX	NX	—	180.0000	10.0000
—	CT	NX	—	0.0000	0.0000
Nonbonding interactions (van der waals) <sup>a</sup>		$R_{ii}^*$ (Å) <sup>b</sup>	$\epsilon_{ii}$ (kcal mol <sup>-1</sup> ) <sup>c</sup>		
NR		3.66	0.0690		
OR		3.48	0.0598		
LP		2.00	0.0600		

<sup>a</sup> CX has the same parameters as C in AMBER, NX the same as NB in AMBER [17]

<sup>b</sup>  $R_{ij}^* = (R_i^* + R_j^*)/2$

<sup>c</sup>  $\epsilon_{ii} = (\epsilon_{ii}\epsilon_{jj})^{1/2}$

based on a least-squares fitting of the HF/6-31G\* electrostatic potential, with the addition of a hyperbolic restraint on the charges of non-hydrogen atoms, which allows the reduction of the unphysically high value of the charges of the atoms that are poorly defined by the electrostatic potential (e.g. the atoms buried in the interior of a molecule). It has been shown that this procedure does not seriously impair the quality of the fit of the “pure” quantum mechanically determined ESP [30]. We thus calculated the atomic point charges for six nitroxides according to the RESP procedure: the three compounds under study together with bis(tert-butyl) nitroxide, 2,2,5,5-tetramethyl-3-hydroxypyrrolidine-1-oxyl and 2,2,6,6-tetramethyl-4-piperidinol-1-oxyl (Fig. 2). For each compound the RESP charges were calculated using the unrestricted HF (UHF)/6-31G\* electrostatic potential at the geometries optimized in vacuo at the B3LYP/6-31G\* level.

Inspection of Fig. 2 shows that RESP charges usually have a lower value than the ones calculated by the simple fitting of the electrostatic potential in a Merz–Kollman scheme [31], being much more “appealing” from a physical point of view. For instance, the value of 0.64 au for a carbon atom of the cycle with two methyl substituents is reduced by the RESP procedure to the much

more reasonable value of 0.17 au. At the same time we checked that the RESP charges yield values of the permanent dipole moment in very good agreement with those calculated ab initio.

Since the majority of chemical and biological processes take place in aqueous solution, it is important to determine point charges suitable also for MM electrostatic calculations in water. Moreover, it is surely useful to compare RESP charges obtained at different levels of theory. We then calculated RESP charges at the UHF/6-31G\* and at the B3LYP/6-31G\* levels, both in vacuo and in aqueous solution. A comparison of the results obtained for the six nitroxides, giving four different sets of average “optimum point charges”, is reported in Table 4.

First, it is interesting to ascertain that UHF and B3LYP charges are quite similar suggesting that, due the hyperbolic restraints, RESP charges are less dependent on the level of calculation than charges obtained according to other standard procedures (e.g. Mulliken and Merz–Kollman approaches [31]). Furthermore, charges determined in vacuo at the UHF level are close to B3LYP charges calculated in aqueous solution. Indeed the HF method neglects the contribution to the ground-state wave function of excited electronic configurations in which antibonding molecular orbitals are occupied. Since these molecular orbitals normally have a polarity opposite to that of the corresponding bonding molecular orbitals, HF atomic charges are usually reduced including electron correlation. However polar solvents play an opposite role, favoring charge separation: as

**Fig. 2.** Restrained electrostatic potential charges calculated using the unrestricted Hartree–Fock/6-31G\* electrostatic potential at the geometries optimized in vacuo at the B3LYP/6-31G\* level for six different nitroxides

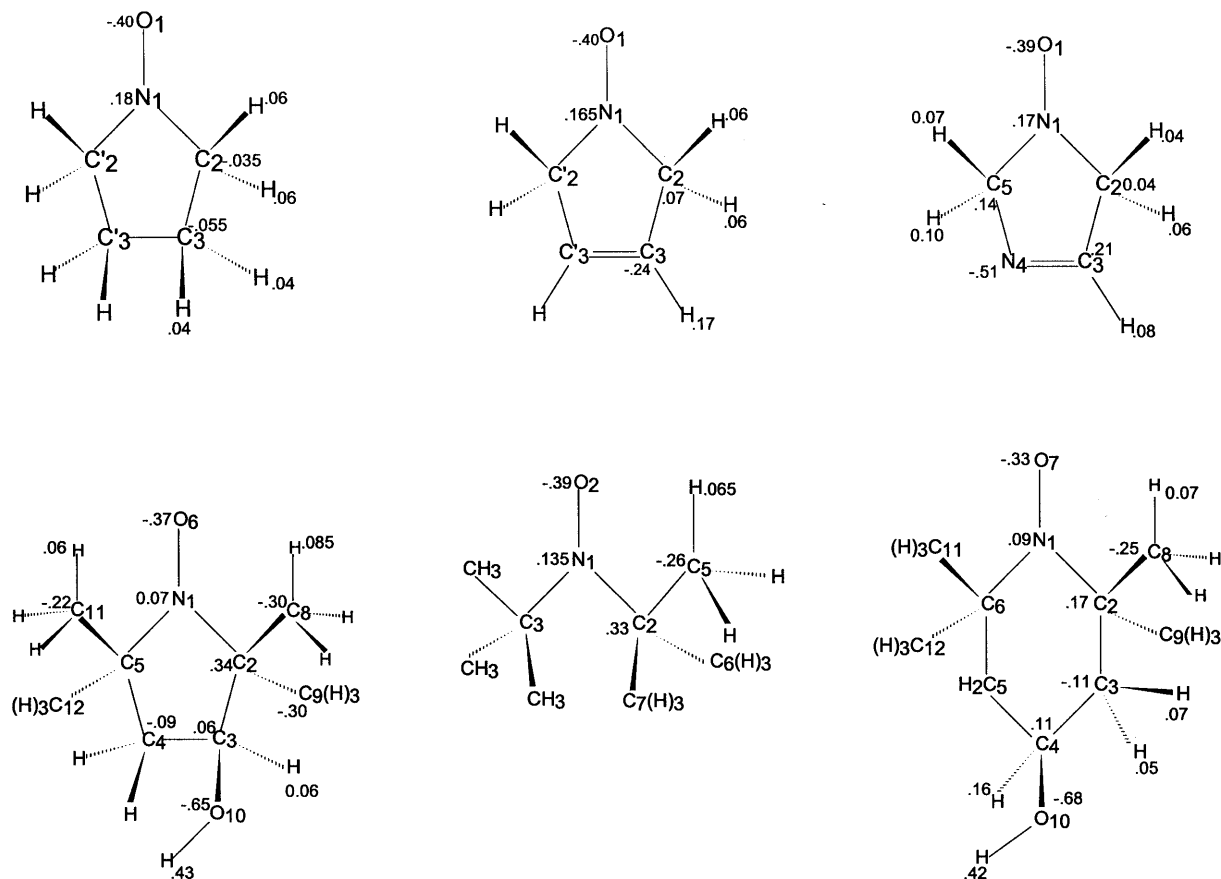


**Table 4.** Atomic point charges based on restrained electrostatic potential charges averaged for the six different nitroxides of Fig. 2 (see text for further details)

	HF/6-31G* in vacuo	HF/6-31G* in water	B3LYP/6-31G* in vacuo	B3LYP/6-31G* in water
N(NO) <sup>a</sup>	+0.135	+0.165	+0.173	+0.192
O(NO) <sup>b</sup>	-0.380	-0.479	-0.399	-0.467
C-NO <sup>c</sup>	+0.151	+0.157	+0.117	+0.119
C <sub>sp</sub> <sup>3</sup> (CH <sub>3</sub> )	-0.257	-0.267	-0.222	-0.231
C <sub>sp</sub> <sup>3</sup> (CH <sub>2</sub> )	-0.084	-0.092	-0.074	-0.080
C <sub>sp</sub> <sup>2</sup>	-0.240	-0.260	-0.200	-0.210
O(OH)	-0.665	-0.733	-0.590	-0.655
H(OH)	+0.425	+0.477	+0.395	+0.455
H-C <sub>sp</sub> <sup>3</sup> <sup>d</sup>	+0.068	+0.074	+0.060	+0.065
H-C <sub>sp</sub> <sup>2</sup> <sup>e</sup>	+0.170	+0.180	+0.140	+0.160

<sup>a</sup> Nitrogen atom of the NO moiety

<sup>b</sup> Oxygen atom of the NO moiety

<sup>c</sup> Carbon atom bound to NO

<sup>d</sup> Hydrogen atom of a methyl group

<sup>e</sup> Hydrogen atom of a methylenic group

a result, charges calculated in solution by post-HF or DFT methods often resemble those calculated in vacuo at the HF level.

The NO moiety represents a remarkable exception, since the unpaired electron occupies a  $\pi^*$  orbital; thus, any removal of electron density from this orbital by excitation to other antibonding orbitals increases the polarity of the NO bond. This explains why charges calculated at the B3LYP level are now higher than their HF counterparts.

### 3.3 Magnetic properties

The isotropic hfs and the electronic spin density of N1 calculated in vacuo at the B3LYP/EPR-2 level using the geometries optimized either at the AMBER or at the B3LYP/6-31G\* level are compared in the first columns of Table 5. There is very good agreement between both sets of results, confirming the reliability of the geometry calculated at the AMBER level. The most remarkable discrepancy (0.8 G) concerns species III and is due to the slightly larger pyramidalization of the NO moiety predicted by the B3LYP geometry optimizations (Table 3).

The hyperfine coupling constants can indeed be decomposed into two contributions [28]: a delocalization term, which is the direct contribution of the nominally unpaired orbital, and a spin polarization (or indirect) contribution, which arises from the interactions of the  $\sigma$  skeleton electrons with the unpaired spin electron. When the NO moiety is planar, the singly occupied molecular

orbital (SOMO) is a pure  $\pi$  orbital and the nitrogen atom lies in its nodal plane: as a consequence the delocalization term vanishes and only the indirect effect contributes to  $A_N$ . On the other hand, pyramidalization of the NO moiety increases the  $s$  character of the SOMO, leading to a nonvanishing delocalization contribution to the hfs and increasing the value of  $A_N$ .

These considerations can also explain why the trend in the hfs exhibited by the three compounds examined does not parallel the relative variation of the calculated spin density at N1.

An increase in the electronegativity of the  $\beta$  atom of the ring obviously disfavors the resonance structure shown in Fig. 3b (which implies a positively charged nitrogen atom) and leads to a decrease in the spin density at the nitrogen. Notwithstanding this, in I and II the NO moiety is planar and the calculated hfs are thus lower than in III, in which the geometry at N1 is partially pyramidal. When, as in the 2,2,5,5-tetramethylated derivative compounds, the geometry of NO is forced to be planar, the polarization term (proportional to the spin density) makes the hfs increase in the order III < II < I in full agreement with the experimental results [32–35].

The next step in our analysis was the evaluation of the solvent effect on the magnitude of  $A_N$  for compounds I–III. To the best of our knowledge, experimental data are available for I and just in two solvents, CH<sub>2</sub>Cl<sub>2</sub> (14.9 G) [33] and water (16.7) [34]. Assuming that for I the behavior of the variation of  $A_N$  with the solvent parallels that determined for similar compounds, the extrapola-

**Table 5.** Isotropic hyperfine splitting ( $A_N$  in gauss) of nitroxide nitrogen calculated in vacuo at the B3LYP/EPR-2/AMBER level and solvent shifts for the passage to an aqueous solution

Compound	Nitrogen spin density in gas phase	$A_N$ gas phase	$\Delta A_N$ PCM	$\Delta A_N$ Adduct	$\Delta A_N$ Adduct + PCM	$\Delta A_N$ Exp
I	0.454 (0.456) <sup>a</sup>	8.08 (8.24) <sup>a</sup>	+1.64	+1.55	+2.48	$\approx 2.50$ <sup>b</sup>
II	0.453 (0.451) <sup>a</sup>	8.20 (8.20) <sup>a</sup>	+1.61	+1.56	+2.59	2.00 <sup>c</sup>
III	0.443 (0.432) <sup>a</sup>	8.49 (9.32) <sup>a</sup>	+1.71	+1.73	+3.11	

<sup>a</sup> The values in parentheses are obtained using B3LYP/6-31G\* geometries

<sup>b</sup> Calculated spin densities for the NO nitrogen estimated from the values of Refs. [33, 34]

<sup>c</sup> Solvent shift *n*-hexane water for the compound 2,2,5,5-tetramethyl-3-carboxy-pyrroline-1-oxyl [7]

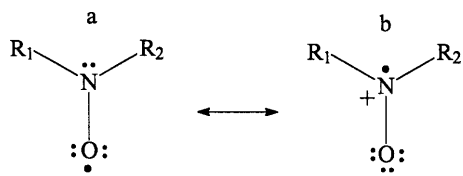


**Fig. 3a, b.** The two most stable resonance structures of a nitroxide free radical

tion of the data gives a solvent shift of about 2.5 G for the passage from the gas phase to an aqueous solution. The reliability of this value is supported by the solvent shift of  $A_N$  for 2,2,5,5-tetramethylated derivatives of I, which is 2.35 G going from dodecane to water [35].

Firstly, we evaluated the effect of the bulk properties of the solvent (such as the dielectric constant), calculating  $A_N$  for every compound using the wave function determined in aqueous solution from the PCM. The results reported in the third column of Table 5 show that a polar embedding medium stabilizes the resonance structure (Fig. 3b) and increases the magnitude of  $A_N$ , in agreement with the experimental results; however the predicted solvent shift is remarkably smaller than the experimental estimates, suggesting that it is necessary to take into account the role played by the interactions between the nitroxide moiety and specific solvent molecules. As a matter of fact, spectroscopic observations clearly show that two water molecules are strongly and specifically bound to the nitroxide oxygen [36].

We then optimized the intermolecular parameters of adducts formed by the nitroxides and two water molecules at the MM level; the corresponding  $A_N$  were then evaluated at the B3LYP/EPR-2 level both in the gas phase and in aqueous solution. The geometries of the three adducts (Fig. 1) are similar to those optimized at the B3LYP/6-31G\* level, but for slightly shorter bond distances (0.05 Å) between the oxygen of the NO moiety and the hydrogen atom engaged in the hydrogen bond (Hw) and a larger Hw—O1—N1 bond angle. It is worth noting that in order to obtain reasonable structures of the adducts it was necessary to explicitly define lone pairs for the nitroxide oxygen [13]. The effect of the hydrogen bonding in the gas phase is rather small, whereas the simultaneous inclusion of the bulk effect and of specific interactions leads to computed solvent shifts in good agreement with the experimental results and with those obtained by B3LYP geometry optimizations.

#### 4 Conclusions

We have extended the AMBER force field to open-chain and cyclic nitroxides, also containing a protonable site (namely the nitrogen atom N2 in III). These nitroxides are particularly interesting as “spin probes” because their  $A_N$  depends remarkably on the pH of the embedding medium, allowing a high-precision measurement of pH and of its gradient in important biological systems, such as cellular membranes, vesicles and

micelles. In this context, our results show that the geometries optimized by the AMBER force field are also reliable for the B3LYP/EPR-2 calculation of the EPR parameters of nitroxides both in vacuo and in solution.

From another point of view the average atomic charges presented in Table 4 should allow reliable MM calculations of the electrostatic interaction in a wide range of nitroxides, both in vacuo and in aqueous solution: they were indeed obtained on the grounds of a representative set of nitroxides, including both linear and cyclic (and heterocyclic) compounds, with substituents of different bulkiness and different ranges of pyramidalization of the NO group. Moreover, the magnitude of the RESP charges exhibits small fluctuations in similar functional groups and the charges (which are not very dependent on the level of calculation) are in agreement with chemical intuition, though reflecting the effect of local variations in a realistic and no arbitrary way. The HF RESP charges calculated in vacuo are rather suitable also for electrostatic calculations performed in aqueous solution, except for the NO moiety, whose peculiar electronic structure can be described only by more sophisticated QM models.

A number of computations confirmed that in aqueous solution it is necessary not only to take into account the macroscopic properties of the bulk solvent but also to correctly describe the features of the cybotactic region of the solvent (such as the effect of hydrogen bonding between the NO group and H<sub>2</sub>O molecules). From this point of view, only the introduction of explicit lone pairs in the AMBER force field leads to a correct description of the basic adduct between the NO moiety and two water molecules.

Thus, the present work represents another step towards the implementation of effective and reliable QM/MM methods for the study of large nitroxide systems and of their interactions with macromolecular systems (proteins, micelles) of biological interest.

#### References

- Rassat A (1990) *Pure Appl Chem* 62: 223
- Ricca A, Tronchet JM, Weber J, Ellinger Y (1992) *J Phys Chem* 96: 10779
- (a) Berliner LJ (ed) (1976) *Spin labeling: theory and applications*. Academic, New York; (b) Griffith OH, Waggoner AS (1969) *Acc Chem Res* 2: 17; (c) Stone TJ, Buckham T, Nordio PL, McConnell HM (1965) *Proc Natl Acad Sci USA* 54: 1010; (d) Keana JFW (1978) *Chem Rev* 78: 37
- (a) Bales BL, Messina L, Vidal A, Peric M, Nascimento OR (1998) *J Phys Chem* 102:10347; (b) Almeida LE, Borissevitch IE, Yushmanov VE, Tabak M (1998) *J Colloid Interface Sci* 203: 456
- Berliner LJ, Reuben J (eds) (1989) *Biological magnetic resonance*, vol 8. Plenum, New York
- Keana JFW, Acarregui MJ, Boyle SLM (1982) *J Am Chem Soc* 104: 827
- (a) Knauer BR, Napier JJ (1976) *J Am Chem Soc* 98: 4395; (b) Reddoch AH, Kinishi S (1979) *J Chem Phys* 70: 2121; (c) Abe T, Tero-Kubota S, Ikegami Y (1982) *J Phys Chem* 86: 1358
- Baglioni P, Ottaviani MF, Martini G, Ferroni E (1984) In: Mittal KL, Lindman B (eds), *Surfactants in solution*, vol 1. Plenum, New York, p 542

9. Baglioni P, Rivara-Minten E, Dei L, Ferroni E (1990) *J Phys Chem* 94: 8218
10. Buhre LMD, Rupert LAM, Engherts JBFN (1988) *Recl Trav Chim Pays-Bas* 107: 17
11. Kang YS, Kevan L (1994) *J Phys Chem* 98: 7264
12. Lajzerowicz-Bonneteau J (1970) In: *Spin labeling: theory and applications*. Academic, New York, p 230
13. Barone V, Bencini A, Cossi M, di Matteo A, Mattesini M, Totti F (1998) *J Am Chem Soc* 120: 7069
14. (a) Barone V, Capecchi G, Brunel Y, Dheu Andries ML, Subra R (1997) *J Comput Chem* 117: 5179; (b) Barone V (1994) *J Chem Phys* 101: 10666
15. (a) Amovilli C, Barone V, Cammi R, Cancès E, Cossi M, Mennucci B, Pomelli C, Tomasi J (1998) *Adv Quantum Chem* 32: 227; (b) Rega N, Cossi M, Barone V (1997) *J Am Chem Soc* 119: 12962
16. Barone V, Cossi M, Tomasi J (1997) *J Chem Phys* 107: 3210
17. Cornell WD, Cieplak P, Bayly CI, Gould IR, Merz KM Jr, Ferguson DM, Sellmayer DC, Fox T, Caldwell JW, Kolmann PA (1995) *J Am Chem Soc* 117: 5179
18. Parr RG, Yang W (1989) *Density functional theory of atoms and molecules*. Oxford University Press, New York
19. Barone V (1995) In: Chong DP (ed) *Recent advances in density functional methods*. World Scientific, Singapore, p 287
20. (a) Becke AD (1988) *Phys Rev B* 38: 3098; (b) Lee C, Yang W, Parr RG (1988) *Phys Rev B* 37: 785
21. Foresman JB, Frisch AE (1996) *Exploring chemistry with electronic structure methods*, 2nd edn. Gaussian, Pittsburgh, Pa
22. Adamo C, Barone V, Fortunelli A (1995) *J Chem Phys* 102: 384
23. Weltner W (1989) *Magnetic atoms and molecules*. Dover, New York
24. Frisch MJ, Trucks GW, Schlegel HB, Scuseria GE, Robb MA, Cheeseman JR, Zakrzewski VG, Montgomery JA, Stratmann RE, Burant JC, Dapprich S, Millam JM, Daniels AD, Kudin KN, Strain MC, Farkas O, Tomasi J, Barone V, Cossi M, Cammi R, Mennucci B, Pomelli C, Adamo C, Clifford S, Ochterski J, Petersson GA, Ayala PY, Cui Q, Morokuma K, Malick DK, Rabuck AD, Raghavachari K, Foresman JB, Cioslowski J, Ortiz JV, Stefanov BB, Liu G, Liashenko A, Piskorz P, Komaromi I, Gomperts R, Martin RL, Fox DJ, Keith T, Al-Laham MA, Peng CY, Nanayakkara A, Gonzalez C, Challacombe M, Gill PMW, Johnson B, Chen W, Wong MW, Andres JL, Head-Gordon M, Replogle ES, Pople JA (1998) *Gaussian 98*. Gaussian, Pittsburgh, Pa
25. Hyperchem, release 4.5 for Windows (1995) Hypercube, Waterloo, Ontario, Canada
26. Chion B, Lajzerowicz J (1968) *Acta Crystallogr B* 24: 196
27. Boeyens JCA, Kruger GJ (1970) *Acta Crystallogr B* 26: 668
28. (a) McConnell HM, Chesnut DB (1958) *J Chem Phys* 28: 107; (b) Barone V, Subra R (1996) *J Chem Phys* 104: 2630; (c) Barone V, Adamo C, Brunel Y, Subra R (1996) *J Chem Phys* 105: 3168
29. Sakakibara K, Kawamura H, Nagata T, Ren J, Hirota M, Shimazaki K, Chemna T (1994) *Bull Chem Soc Jpn* 67: 2768
30. Bayly CI, Cieplak P, Cornell WD, Kollman PA (1993) *J Phys Chem* 97: 10269
31. Basler BH, Merz KM Jr, Kolmann PA (1990) *J Comput Chem* 11: 431
32. Khrantsov VV, Weiner LM, Grigoriev IA, Volodarsky LB (1982) *Chem Phys Lett* 91: 69
33. Chapelet-Letourneux G, Lemaire H, Rassat A (1965) *Bull Soc Chim Fr* 3283
34. Hudson A, Hussain HA (1968) *J Chem Soc B* 251
35. Keana JFW, Lee TD, Bernard EM (1976) *J Am Chem Soc* 98: 3052
36. Symons MCR, Pena-Nuñez A (1985) *J Chem Soc Faraday Trans 1* 81: 2421